

# DFT Study of Small Palladium Clusters Pd<sub>n</sub> and Their Interaction with a CO Ligand ( $n = 1-9$ )

Giuseppe Zanti<sup>[a]</sup> and Daniel Peeters<sup>\*[a]</sup>

**Keywords:** Cluster compounds / Palladium / Carbonyl ligands / Density functional calculations

This paper presents a theoretical study of palladium clusters Pd<sub>n</sub> of low nuclearity, ranging from 1 to 9, completed by their interactions with a carbonyl ligand (Pd<sub>n</sub>CO). The simulations were performed at the DFT (B3LYP–Lanl2DZ) level. Small palladium clusters are deltahedral structures characterized by a triplet ground state (Pd<sub>2</sub> to Pd<sub>7</sub>) or a quintet ground state for larger nuclearities (Pd<sub>8</sub> and Pd<sub>9</sub>). Various electronic states relatively close in energy are present. These states have close geometries but differ by their electron density distribution. A significant electronic population of the 5s orbital is needed to explain the existence and cohesion of palladium–palladium bonds. These latter are formed by the combination of sd hybrid orbitals and get stronger as the 5s character increases. The relative stability of palladium clusters increases with their nuclearity and the study of fragmentation reactions

shows a particular stability of Pd<sub>4</sub>, Pd<sub>6</sub> and Pd<sub>9</sub> clusters. The adsorption of the CO ligand goes through a back-bonding interaction favoured by a high 4d and a low 5s atomic population. This interaction therefore affects the metal–metal bond and the ground state of the cluster becomes a singlet for the first members of the series. The favoured coordination mode is one that maximizes the back-bonding interaction, i.e. the capped position ( $\mu_3$ ) on a cluster's face. However, stabilization provided by the presence of one ligand at the expense of a large number of metal–metal bonds is not sufficient and, in the case of larger clusters, a triplet ground state remains.

(© Wiley-VCH Verlag GmbH & Co. KGaA, 69451 Weinheim, Germany, 2009)

## Introduction

Metal clusters considered as molecular entities formed by assembling a small number of atoms, ranging from a few to several hundreds, are now an important issue in the fields of nanotechnology and catalysis. Their defined composition and geometry confer to specific electronic and unique energetic properties of metal clusters that distinguish them clearly from the corresponding metal bulk.<sup>[1]</sup> These properties generally vary with the size and composition of the system. Currently, a large number of synthesis strategies of metal clusters are known and can be grouped into two distinct categories. On the one hand, one finds physical methods such as condensation of atomic vapour and molecular beams.<sup>[2]</sup> These usually bare clusters are produced in small quantities and have a short lifetime. Characterizing their structural properties and controlling their size (nuclearity) is generally difficult. On the other hand, one finds chemical methods such as the reduction of metallic salts in solution. A protective sphere of ligands surrounds the metallic core

and stabilizes the clusters produced by these methods. The latter allows an easier structural characterization, resting on conventional analytical techniques such as IR and NMR spectroscopy or X-ray crystallography.<sup>[3]</sup>

This work has focused on a detailed theoretical study of palladium clusters with a nuclearity ranging from 2 to 9 (Pd<sub>n</sub>;  $n = 2-9$ ) and on their interaction with a  $\pi$ -acceptor ligand, in this case CO (Pd<sub>n</sub>CO). The choice of the carbonyl ligand is justified by the fact that it is commonly used in the synthesis of palladium clusters.<sup>[3]</sup> In addition to this, smaller systems (Pd, Pd<sub>2</sub> and Pd<sub>3</sub>) may serve as models to study the adsorption of the ligand on a vertex, an edge and a face of palladium clusters, respectively. If a large number of theoretical papers are already devoted to the study of these compounds, they generally focus on the determination of the geometry of the ground state. To this end, palladium clusters have been simulated by a wide range of methods, ranging from “simple” semi-empirical methods,<sup>[4,5]</sup> to the most complex post-SCF methods,<sup>[6,7]</sup> as well as density functional theory (DFT).<sup>[8–12]</sup> Recently, palladium clusters with larger nuclearity were also studied by molecular dynamics.<sup>[13]</sup> Interactions of ligands with the metal core have also been the subject of a series of works which include, among others, interactions with CO,<sup>[14,15]</sup> NO,<sup>[16]</sup> S and Cl,<sup>[17]</sup> O<sub>2</sub><sup>[18]</sup> or H and CH<sub>x</sub>.<sup>[19]</sup> In this work, we intend to push further the investigation of these species by addressing in greater detail their electronic structure. Such a descrip-

[a] Unité de Chimie Structurale et des Mécanismes Réactionnels, Département de Chimie, Université Catholique de Louvain, Bâtiment Lavoisier, Place Louis Pasteur 1, 1348 Louvain-la-Neuve, Belgium  
Fax: +32-10-47-27-07  
E-mail: daniel.peeters@uclouvain.be

Supporting information for this article is available on the WWW under <http://dx.doi.org/10.1002/ejic.200900513>.

tion should lead to a better understanding of catalytic properties. To this end, calculations of density isocontours help to provide a better perception of the electronic reorganization that takes place during the formation of clusters from free atoms but also of the electronic exchange involved by the adsorption of CO on the metal cluster. Natural population analyses are fruitful in quantifying those effects. Further, structural, electronic, and energetic properties are compared and discussed with or without CO in the cluster. Finally, the stability of palladium clusters has been addressed through a selection of fragmentation reactions that may occur during the nucleation process. After presenting a short survey of the methodology used and the difficulties encountered during the optimization process, we shall report and discuss the results. The discussion is further divided into two parts. The first part, where we discuss the electronic structure for the smaller clusters ( $\text{Pd}_{1-3}$ ), compares bare clusters ( $\text{Pd}_n$ ) and monocarbonyl clusters ( $\text{Pd}_n\text{CO}$ ). The second part generalizes the obtained conclusions to the next members of this series ( $n = 4-9$ ). In this part, we will also study the evolution of some energy properties such as relative stabilities and ligand adsorption energies with cluster size. Finally, the conclusion will summarize the main points of our study and outline some perspectives.

## Methodology and Precautions

As transition metal clusters present a great number of electrons, which reorganize deeply the atomic electron density, we decided to simulate palladium clusters using the density functional theory (DFT<sup>[20]</sup>) which, given the earlier work,<sup>[11,12]</sup> seems to provide consistent results. This allows to introduce some of the electronic correlation required to study such systems, while maintaining a good ratio of quality to computing time. On the one hand, we opted for the exchange–correlation hybrid functional B3LYP.<sup>[21]</sup> On the other hand, treating metal clusters requires choosing an appropriate basis set, capable of providing sufficient flexibility to describe as faithfully as possible electronic relocation while limiting the number of electrons and maintaining computations in an affordable time. These reasons led us to choose the Lanl2DZ basis set,<sup>[22–24]</sup> which deals explicitly with electrons in the outer layers through a split valence polarized basis set, retaining thus 18 electrons per Pd atom ( $4s^2 4p^6 4d^{10}$ ), while the remaining electrons are modelled through an effective core potential taking into account some relativistic corrections (RECP). C. Xiao and co-workers studied the relativistic effects on geometry and electronic structure of small  $\text{Pd}_n$  species.<sup>[25]</sup> Regarding the carbonyl ligand, the classical extended 6-31G(d,p) basis set<sup>[26]</sup> was used. Finally, the distribution of the electronic population has been analyzed through the NBO natural population analysis.<sup>[27,28]</sup> All computations and geometry optimizations were carried out using the Gaussian 03 package.<sup>[29]</sup>

As the number of possible structural isomers grows exponentially with the size of the cluster, it is essential to establish a strategy for exploring the different local potential en-

ergy surfaces (PES) that we will consider. In our approach, we have simulated the palladium clusters from a wide variety of predefined geometries based on the various symmetry point groups. We took care, however, to release the full symmetry during the optimization processes in order to allow for structural distortions and introduce any stabilizing effect, which may affect the system (for example a Jahn–Teller effect). Another question to be raised concerns the spin multiplicity. Because the palladium atom presents a closed-shell electronic configuration ( $4d^{10}$ ), part of its 4d electronic density must necessarily be promoted into the nearest orbitals, in this case 5s, to enable the formation of a stable metal–metal bond. Consequently, all structures have been optimized for the various accessible spin multiples, i.e. singlet and triplet states, even quintet for the last clusters of the series. Even though we will focus on the ground states, a series of optimizations was carried out in the quintet state for clusters of larger nuclearity ( $n = 7-9$ ). Let us finally note that the large number of d electrons usually leads to a wide variety of closely lying electronic states (“low-lying states”). We must mention here that Balasubramanian carried out a detailed MCSCF study of such low-lying states for the smallest palladium clusters ( $\text{Pd}_2$ ,<sup>[30]</sup>  $\text{Pd}_3$ ,<sup>[31]</sup> and  $\text{Pd}_4$ <sup>[32]</sup>). The proximity of such states can be misleading, as crossings between potential energy surfaces can occur at various points, making optimizations somewhat difficult. In other words, the geometry of the starting point selects a PES, which may be different from the hypersurface related to the ground electronic state. This often induces the localization of a minimum that is not located on the ground PES. We will not go into the details of this problem here, as it will be the object of a forthcoming publication. Nevertheless, to ensure that each identified extremum belongs to its lowest energy electronic state we have adopted the following strategy:

- (1) a stability test of the electronic density was achieved for an each spin multiplicity
- (2) an analysis of the energy second derivative confirms that, among all obtained extrema, the real minimum has been attained, or eventually a first-order saddle point identified, when the transition state presents some chemical interest.

Caution must be taken in the analysis of the results, and this explains why some published structures and energies may differ from one paper to another even when identical methods and functionals are used.

## Results and Discussion

To introduce the discussion, we will in this section present the global results obtained for the bare clusters ( $\text{Pd}_n$ ;  $n = 1-9$ ) and their monocarbonyl complexes ( $\text{Pd}_n\text{CO}$ ). The stability of palladium clusters is usually discussed in terms of binding energies  $\Delta E_B$  and cohesive energies  $\Delta E_C$ , which are defined by Equations (1) and (2).

$$\Delta E_B = -(E_{\text{Pd}_n} - n E_{\text{Pd}}) \quad (1)$$





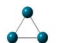







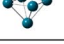


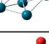


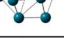






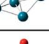






$$\Delta E_C = \Delta E_B/n \quad (2)$$

$E_{\text{Pd}_n}$  is the energy of  $\text{Pd}_n$  cluster and  $E_{\text{Pd}}$  refers to the atomic ground state ( $^1\text{S}$ ). Cohesive energies normalize the binding information and allow an easy comparison of the stability acquired by the various nuclearities. For the monocarbonyl complexes, the gain in stability provided by the adsorption of the CO ligand on the cluster  $\Delta E_{\text{ads}}$  can be calculated as the energy difference between the complex and the isolated partners [Equation (3)].

$$\Delta E_{\text{ads}} = E_{\text{Pd}_n\text{CO}} - (E_{\text{Pd}_n} + E_{\text{CO}}) \quad (3)$$

Table 1 collects the data for the various clusters considered in this paper. It incorporates the global minimum for each size of bare palladium clusters as well as some close local minima. Because the number of structural isomers increases rapidly with the cluster size, we present only a few selected structures that correspond to lowest minima. The different clusters are given with their symmetry, ground spin multiplicity, and cohesive energies. The energy difference between the ground state and local minima is given in the last column  $\Delta E_f$ . Table 1 presents also the most pertinent results obtained for the monocarbonyl complexes in their ground state. The CO frequency being a very sensitive prop-

Table 1.  $\text{Pd}_n$  clusters and their monocarbonyl complexes (PGS: point group symmetry; SM: spin-multiplicity;  $\Delta E$  are in kcal/mol).

| $n$ | $\text{Pd}_n$   | PGS            | SM | $\Delta E_C$ | $\Delta E_f$ | $\text{Pd}_n\text{CO}$  | CM              | SM | $\Delta E_{\text{ads}}$ | $d_{\text{Pd-CO}}$<br>[Å] | $d_{\text{C-O}}$<br>[Å] | $\nu_{\text{CO}}$<br>[cm <sup>-1</sup> ] | $2 p^*_{\text{CO}}$<br>[e <sup>-</sup> ] |
|-----|---|----------------|----|--------------|--------------|---|-----------------|----|-------------------------|---------------------------|-------------------------|--|--|
| 1   |    | —              | 1  | —            | —            |    | $\mu_1$         | 1  | -44.56                  | 1.87                      | 1.15                    | 2129                                     | 0.31                                     |
| 2   |    | $D_{\infty h}$ | 3  | 11.07        | —            |    | $\mu_2$         | 1  | -61.72                  | 1.96                      | 1.17                    | 1959                                     | 0.56                                     |
| 3   |    | $C_{2v}$       | 3  | 19.66        | —            |    | $\mu_3$         | 1  | -62.46                  | 2.03                      | 1.19                    | 1839                                     | 0.74                                     |
| 4   |    | $C_{3v}$       | 3  | 28.80        | —            |    | $\mu_3$         | 1  | -43.02                  | 2.01                      | 1.20                    | 1789                                     | 0.81                                     |
| 5   |   | $D_{3h}$       | 3  | 30.51        | 0.00         |   | $\mu_3$         | 1  | -38.88                  | 2.01                      | 1.20                    | 1782                                     | 0.82                                     |
|     |  | $C_{4v}$       | 3  | 29.99        | 2.60         |  | $\mu_3$<br>(TS) | 1  | -36.72                  | 1.99                      | 1.20                    | 1767                                     | 0.83                                     |
| 6   |  | $D_{4h}$       | 3  | 32.52        | —            |  | $\mu_2$         | 3  | -37.13                  | 1.99                      | 1.17                    | 1962                                     | 0.51                                     |
| 7   |  | $C_2$          | 3  | 33.19        | 0.00         |  | $\mu_2$         | 3  | -42.42                  | 2.02                      | 1.17                    | 1963                                     | 0.51                                     |
|     |  | $C_s$          | 3  | 32.86        | 2.32         |  | $\mu_2$         | 3  | -46.70                  | 1.98                      | 1.17                    | 1943                                     | 0.54                                     |
| 8   |  | $C_8$          | 5  | 33.84        | 0.00         |  | $\mu_3$         | 3  | -48.47                  | 2.04                      | 1.19                    | 1824                                     | 0.73                                     |
|     |  | $C_2$          | 5  | 33.80        | 0.34         |  | $\mu_3$         | 3  | -46.44                  | 2.03                      | 1.19                    | 1809                                     | 0.76                                     |
|     |  | $D_{2d}$       | 3  | 33.76        | 0.61         |  | $\mu_2$         | 3  | -46.18                  | 1.99                      | 1.17                    | 1957                                     | 0.53                                     |
|     |  | $C_s$          | 5  | 33.70        | 1.12         |  | $\mu_2$         | 3  | -46.27                  | 1.98                      | 1.17                    | 1948                                     | 0.53                                     |
| 9   |  | $C_3$          | 5  | 35.26        | 0.00         |  | $\mu_2$         | 5  | -37.68                  | 1.99                      | 1.17                    | 1942                                     | 0.53                                     |
|     |  | $C_2$          | 5  | 34.72        | 4.84         |  | $\mu_2$         | 5  | -45.91                  | 1.99                      | 1.17                    | 1950                                     | 0.52                                     |
|     |  | $C_2$          | 5  | 34.61        | 5.82         |  | $\mu_2$         | 5  | -42.45                  | 1.98                      | 1.17                    | 1952                                     | 0.52                                     |

erty, its variation measures the perturbation induced to the carbonyl bond by the adsorption phenomenon. The corresponding wave number reported in the Table is computed from the optimized structure at the harmonic approximation level. Structural data such as Pd–CO and CO bond lengths are also given. Finally the electronic population of the antibonding  $\pi^*_{\text{CO}}$  orbital is also given. It is out of the scope of this paper to publish extensively the structural data of the studied species, they are nevertheless given in the Supporting Information file associated to this work.

Palladium clusters with nuclearity between 2 and 9 adopt preferentially deltahedral compact structure with a spin-multiplicity that increases with the size of the system. The smaller clusters with  $n$  between 2 and 7 present a triplet ground state while the  $\text{Pd}_8$  and  $\text{Pd}_9$  are most stable in the quintet state. These geometrical and electronic trends are consistent with works conducted previously<sup>[8–12]</sup> but the quintet state becomes more stable than the triplet state from  $\text{Pd}_8$  rather than from  $\text{Pd}_9$ . This may be due to the use of another functional and another basis set, as the difference between these two electronic states remains small for  $\text{Pd}_8$  (0.61 kcal/mol). One must point out at this stage is that when multiple low-energy structures are obtained, the energy differences are usually very small, suggesting that at room temperature a mixture of such structures should be obtained, which makes it difficult to attribute a definite structure to the cluster. Generally, the link between these geometries is a simple movement along a normal coordinate passing through a low energy transition state.

We will focus first on the three first palladium clusters ( $\text{Pd}_{1-3}$ ) and analyse in some more detail their electronic structure and binding properties while the extension of the analysis to the larger clusters will be considered afterwards, in the second part.

### (a) $\text{Pd}_n$ and $\text{Pd}_n\text{CO}$ for $n$ Ranging from 1 to 3

In his ground state, the palladium atom presents a closed-shell electronic configuration  $4d^{10}$  ( $^1\text{S}$ ). In order to make stable Pd–Pd bonds, the contribution of the 5s orbital to the electronic density is required. From the “atom in molecule” point of view, this would correspond to a  $4d^{10-x}5s^x$  electronic configuration ( $0 \leq x \leq 1$ ), which can be justified from a perturbation viewpoint by the mixture of  $4d^{10}$  and  $4d^95s^1$  states. A computation shows that the latter triplet electronic configuration lies 19.8 kcal/mol above the ground state, which remains relatively close to the experimental value of 21.6 kcal/mol.<sup>[10]</sup> The proximity of those electronic configurations justifies their mixture in describing the complex electronic structure of the metal cluster. The  $4d^85s^15p^1$  state is located significantly higher in energy and, at first approximation, can be ignored in the electronic description of small palladium clusters. Note that the introduction of relativistic corrections is essential to getting consistent results.<sup>[33]</sup>

The addition of the  $\pi$ -acceptor CO ligand on a palladium atom stabilizes the system by a  $\sigma$ -donation  $\pi$ -back-donation mechanism (“back-bonding”). The stabilization effect is due, on the one hand, to the donation of the  $\sigma$ -type lone pair of CO in the low-lying empty s orbital of Pd and, on the other hand, to the back-donation of d electrons of Pd into the  $\pi$ -type antibonding orbitals of CO. We can quantify these interactions energetically and electronically by  $\Delta E_{\text{ads}}$  and the natural orbital analysis, respectively. The theoretical data for the PdCO complex are shown in Table 3. The energy released during the adsorption of the CO ligand on the Pd atom is 44.56 kcal/mol (not corrected for difference ZPVE). This value is slightly greater than that obtained by more complex methods [CCSD(T), QCISD(T)].<sup>[33]</sup> The intensity of back-bonding results in the relocation of 0.3 electron from the orbital  $4d_{xz}$  and  $4d_{yz}$  of the palladium atom to the  $\pi^*$  empty orbitals of the CO. This interaction is illustrated in Figure 1 (a) through a graph of differential density contours. We can also see in this figure a reduction of the electronic density along the Pd–CO axis, which can be explained by a repulsion between the lone pair of the carbonyl and the  $4d_{z^2}$ –5s electrons of palladium. The degree of interaction can be also verified by the weakening of the C–O bond resulting from the electronic settlement of its  $\pi^*$  antibonding orbitals. The increase in C–O bond length and the decreasing in frequency of its “stretching” are characteristics of a terminal coordination ( $\mu_1$ ). Structural data referenced in the Table 3 are in good agreement with the experimental data ( $d_{\text{Pd-C}} = 1.843$  and  $d_{\text{C-O}} = 1.138$  Å).<sup>[34]</sup> Our results are slightly higher ( $d_{\text{Pd-C}} = 1.867$  and  $d_{\text{C-O}} = 1.151$  Å) but only more complex methods allow reaching them.<sup>[33]</sup>

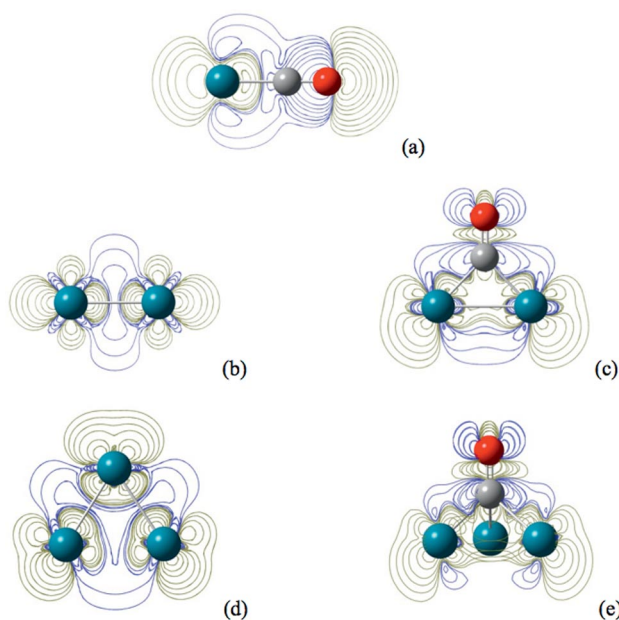


Figure 1. Differential density isocontours for the PdCO (a),  $\text{Pd}_2$  (b),  $\text{Pd}_2\text{CO}$  (c),  $\text{Pd}_3$  (d) and  $\text{Pd}_3\text{CO}$  (e) ( $1 \cdot 10^{-3} e^-/\text{bohr}^3$ ).



Table 2. Data concerning the Pd<sub>2</sub> dimer in its singlet and triplet states.

|                                      | Bond length [Å] | $\nu$ Stretch. [cm <sup>-1</sup> ] | $\Delta E_B$ [eV]           | Atomic pop. [e <sup>-</sup> ] |
|--------------------------------------|-----------------|------------------------------------|-----------------------------|-------------------------------|
| Pd <sub>2</sub> exp.                 | 2.4–2.5         | 210 <sup>[35]</sup>                | 1.03 ± 0.16 <sup>[36]</sup> | –                             |
| <sup>3</sup> Pd <sub>2</sub> (B3LYP) | 2.53            | 204                                | 0.96                        | 4d (9.41) 5s (0.58)           |
| <sup>1</sup> Pd <sub>2</sub> (B3LYP) | 2.76            | 131                                | 0.60                        | 4d (9.90) 5s (0.09)           |

Optimizing the dimer shows a ground triplet state, which is consistent with previous DFT results.<sup>[8–12]</sup> The nearest singlet state is located 8 kcal/mol above. The atomic population analysis justifies this result as we can see a 5s atomic population greater in the case of triplet state, resulting in a larger bonding character. In fact, before bonding can occur, a significant part of the 4d electron density must be promoted in the 5s empty orbital. Indeed, the natural population analysis estimates an occupation of 0.58e<sup>-</sup> for the 5s orbital. The theoretical data concerning the dimer are reported in the Table 2. Because the bonding character is mainly defined from the 5s population, its increase will reduce the bond length, as can be seen by comparing the singlet (2.76 Å) and triplet (2.53 Å) states. These theoretical results are in good agreement with experiment even though the calculated bond length is slightly longer than the experimental value. Differential density curves for the dimer ground state are included in Figure 1b. They suggest an increase of the electronic density around the Pd–Pd axis with a sd-type hybridization.

The system can now be bound by a CO ligand in two ways, either in terminal mode ( $\mu_1$ ) or in bridging mode ( $\mu_2$ ). The calculations were made for the two geometries in the singlet and triplet spin-multiplicities. The results show now that singlet states are lower than the triplet states. This phenomenon is explained by the fact that the density 4d electrons do not have to be promoted to a 5s orbital, as the empty  $\pi^*$  orbital of the CO ligand will accept them. The complex coordinated in terminal mode  $\mu_1$  appeared to be a transition state located 27.5 kcal/mol above the  $\mu_2$  bridging mode. Only the data for the ground  $C_{2v}$  state are shown in Table 3. This result is consistent with the structural study conducted by the group of V. Bertin<sup>[14]</sup> and the group of P. Nava.<sup>[15]</sup> Comparing to PdCO, there is greater charge transfer from 4d orbitals to the  $\pi^*$  orbitals of the CO for the Pd<sub>2</sub>CO complex. Consequently, the CO bond is weaker in the case of the dimer complex (decrease in bond length and increase in stretching frequency). On the other hand, the 5s atomic population decreases in the complex compared to

the bare dimer, which weakens the Pd–Pd bond that becomes longer (2.69 Å). Bonding in Pd<sub>2</sub> requires a 4d<sup>10-x</sup> 5s<sup>x</sup> atomic configuration, whereas binding to CO favours a 4d<sup>10</sup> atomic configuration. The formation of metal–ligand bonds is therefore favoured at the expense of the metal–metal bond. The greater stabilization of the bridging complex releases greater adsorption energy (61.72 kcal/mol) than the PdCO complex, despite the weakening of the metal–metal bond. The differential density contours for the Pd<sub>2</sub>CO complex is illustrated in Figure 1 (c). It clearly shows the “back-bonding” interaction and the conservation of the metal–metal bond. As with the previous complex, the decrease of electronic density in the centre of the structure is partially due to the repulsion caused by the lone pair of the CO ligand.

Trimers were simulated from linear and triangular geometries. The latter are found to be the most stable, while the linear structure corresponds to a transition state. As for dimers, triplet states are located below the singlet states. The difference in energy with the singlet state is about 6 kcal/mol. These trends are also in good agreements with previous works.<sup>[8–12]</sup> It should be noted that a series of similar structures relatively close in energy corresponding to different electronic states have been identified but we do not go into details of these different electronic states here (The ground state corresponds to the <sup>3</sup>B<sub>2</sub> state while the <sup>3</sup>B<sub>1</sub> and <sup>3</sup>A<sub>2</sub> are slightly higher in energy, 0.4 and 1 kcal/mol, respectively). In contrast to the singlet state ( $D_{3h}$ ), which presents a closed-shell configuration higher in energy, the triplet  $D_{3h}$  state shifts to a distorted  $C_{2v}$  geometry (65.5° for the apex angle) due to a Jahn–Teller effect. The electronic ground state is <sup>3</sup>B<sub>2</sub>, as confirmed by K. Morokuma's group.<sup>[37]</sup> The natural population analysis shows that atoms located at the base of the isosceles triangle are characterized by a 5s population less important (0.57e<sup>-</sup>) than the atom located at the top (0.68e<sup>-</sup>). This electronic asymmetry is reflected in structural parameters by introducing a bond length longer at the base (2.76 Å) than the sides of isosceles triangle (2.55 Å). The differential density contours for the ground state is

Table 3. Theoretical data (B3LYP) on complex Pd<sub>n</sub>CO for  $n = 1–3$  and CO ligand.

|   | Pd( $\mu_1$ -CO) ( $C_{\infty v}$ ) | Pd <sub>2</sub> ( $\mu_2$ -CO) ( $C_{2v}$ ) | Pd <sub>3</sub> ( $\mu_3$ -CO) ( $C_{3v}$ ) | CO   |
|---|-------------------------------------|---|---|------|
| $\Delta E_{ads}$ [kcal/mol]             | –44.57                              | –61.72                                      | –62.46                                      | –    |
| $d_{Pd-Pd}$ [Å]                         | –                                   | 2.69  | 2.76  | –    |
| $d_{Pd-C}$ [Å]                          | 1.87                                | 1.96  | 2.03  | –    |
| $d_{C-O}$ [Å]                           | 1.15                                | 1.17  | 1.19  | 1.14 |
| $Q_{Pd}$ [e]                            | 0.05                                | 0.09  | 0.10  | –    |
| $\Delta Q_{CO}$ [e]                     | 0.86                                | 0.75  | 0.64  | 1.00 |
| (4d-5s) <sub>Pd</sub> [e <sup>-</sup> ] | 4d (9.52) 5s (0.43)                 | 4d (9.55) 5s (0.36)                         | 4d (9.58) 5s (0.32)                         | –    |
| 2 $\pi^*_{CO}$ [e <sup>-</sup> ]        | 0.31                                | 0.56  | 0.74  | 0.00 |
| $\nu_{CO}$ [cm <sup>-1</sup> ]          | 2129                                | 1959  | 1839  | 2210 |

shown in Figure 1 (d). The electronic density increases at the centre of the structure and around the bond axis while a decrease is seen on the bond axis.

For the interaction between the trimer and the CO ligand, we can achieve an analysis similar to the dimer. The singlet state, with a lower 5s population and longer Pd–Pd bond lengths, is the ground state. However, the interaction wins in intensity and the variation of structural and electronic parameters is even more important than for the Pd<sub>2</sub>CO complex. Results for Pd<sub>3</sub>CO are listed in Table 3 while differential density contours are shown in Figure 1 (e). Here also, the complex was simulated in its various coordination modes (terminal  $\mu_1$ , bridging an edge  $\mu_2$  or capping a face  $\mu_3$ ). The results show that  $\mu_3$ , with a  $C_{3v}$  symmetry, corresponds to the most stable structure as in this coordination mode the back-bonding interaction is favoured. A notable difference from the previous complex is the adsorption energy, which is quite similar to Pd<sub>2</sub>CO. This is probably because, in this case, three metal–metal bonds are weakened while only one such bond is involved in Pd<sub>2</sub>CO.

### (b) Pd<sub>n</sub> and Pd<sub>n</sub>CO for *n* Ranging from 4 to 9

When the clusters size increases, the optimizations can lead to a relatively large number of structural isomers. For this reason, only the global minimum for each nuclearity and some local minima close in energy are shown in Table 1. From the structural viewpoint, planar structures are much higher in energy than the three-dimensional structures and never correspond to stable minima. All structures are in a triplet ground state, except for Pd<sub>8</sub> and Pd<sub>9</sub>, where a quintet ground state appears. Palladium clusters being characterized by open-shell configurations, a decrease of symmetry by a Jahn–Teller effect can stabilize the system. These results are in good agreement with previously reported DFT results. As a reminder, higher spin-multiplicities are expected when the cluster size increases.<sup>[11,12]</sup>

The most stable structure for Pd<sub>4</sub> is a distorted tetrahedron with a  $C_{3v}$  symmetry. Our results predicted that the linear, square and rhomboid planar structures of Pd<sub>4</sub> would be significantly higher in energy compared to the tetrahedral arrangement for both triplet and singlet multiplicities. Extensive calculations at the multireference configuration interaction with single and double excitations (MRSDCI) level<sup>[32]</sup> confirm this point. Minima with the lowest energy for the three following nuclearities (Pd<sub>5–7</sub>) adopt bipyramidal configurations. The most stable structure for Pd<sub>5</sub> is a trigonal bipyramid with a  $D_{3h}$  symmetry. Unexpectedly, we found another trigonal bipyramid slightly higher in energy but with a  $C_{2v}$  symmetry (0.39 kcal/mol). The square-pyramidal structure is about 2.6 kcal/mol higher than the ground state. These structures were confirmed in the work of K. Morokuma and co-workers at DFT level.<sup>[38]</sup> Note that at this level, it is difficult to determine the ground state of Pd<sub>5</sub> because the relative energy ordering of electronic states differs substantially from one level of theory to an-

other. A large scale of CASSCF and MRSDCI calculations on electronic states of Pd<sub>5</sub> reveal that there are several low-lying electronic states of different geometries for Pd<sub>5</sub>.<sup>[39]</sup> B3LYP calculations for Pd<sub>6</sub> show a distorted octahedron ground state with a  $D_{4h}$  symmetry. The determination of the ground state for Pd<sub>6</sub> is unquestionable as other geometries are significantly higher in energy. This is confirmed by other DFT studies.<sup>[8–12]</sup> For Pd<sub>7</sub>, the most stable structure seems to be the distorted pentagonal bipyramid with a  $C_2$  symmetry. The other structures like capped octahedron and the bi-capped trigonal bipyramid remain very close in energy. At this level, any deltahedral structure leads to a minimum. However, it is more difficult to link these minima on a reaction pathway as they often refer to different electronic states. In addition to the DFT results, a molecular dynamic study confirms the energetic sequence of our structures listed in Table 1 for Pd<sub>7</sub>.<sup>[40]</sup> Pd<sub>8</sub> and Pd<sub>9</sub> adopt three-dimensional structures in the quintet state. For Pd<sub>8</sub>, optimizing the lowest energy structure leads to a structure with a  $C_s$  symmetry while the global minimum calculated for the Pd<sub>9</sub> adopts a configuration with distorted double octahedrons fused with one face. This spin-multiplicity is confirmed in other DFT studies for Pd<sub>9</sub> but there is a doubt for Pd<sub>8</sub>. As it is the case for Pd<sub>5</sub>, Pd<sub>8</sub> seems to present several low-lying electronic states. The use of another functional or another basis set can change the ordering in the sequence of structures listed in Table 1. For example, the BP-86 functional used by the group of P. Nava<sup>[11]</sup> leads to a triplet ground state with a  $D_{2d}$  symmetry, which corresponds to our third structure for the Pd<sub>8</sub> in the Table 1. The difference in energy calculated for these two structures at B3LYP level is very low, only 0.61 kcal/mol.

Regarding the stability of palladium clusters, it can be studied in several ways. The most common is to study the evolution of cohesive energy as given by Equation (2), which depends on the size of the cluster. This evolution is shown in Figure 2 (a). As logically expected, we find that the cohesive energy increases with the cluster size. However, this increase is not constant and is attenuated with the cluster size, tending at limit to an asymptotic behaviour. It can be explained by the fact that the sphere of coordination of palladium atoms tends to a limit as the cluster nuclearity increases. Optimizations with molecular dynamics were carried out for sizes up to 40 atoms<sup>[13]</sup> and show that the limit of the cohesive energy is far from being achieved with a nuclearity of 9. The stability of a cluster with a given nuclearity *n* can also be compared to its closest neighbours (Pd<sub>*n*–1</sub> and Pd<sub>*n*+1</sub>) through fragmentation reactions. These reactions correspond either to the loss of one palladium atom (A) or to the transfer of one atom to another cluster (B).



These reactions bring information about the nuclearities requiring the most important fragmentation energy; it therefore reflects the system stability. The energies  $\Delta E$  of

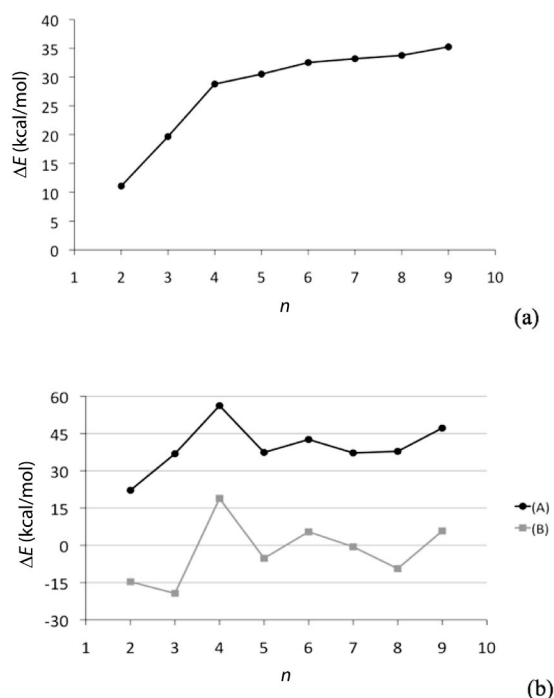


Figure 2. Graphs showing the evolution of energetic properties with the size of palladium clusters: evolution of cohesive energy  $\Delta E_C$  (a), fragmentation energies for reactions A and B (b).

reactions A and B can be visualized on the graph in Figure 2 (b). The theoretical results show a particular stability for  $\text{Pd}_4$  and, to a lesser extent, for  $\text{Pd}_6$  and  $\text{Pd}_9$ . Finally, in contrast to the loss of one palladium atom (A), certain transfers of atoms (B) seem favoured ( $\Delta E < 0$ ) and are without doubt at the origin of cluster nucleation by condensation in the gas phase.

As for smaller clusters, a CO ligand has been added and the structures simulated for the various coordination modes in their singlet, triplet and quintet electronic states. Only the most stable state found for each nuclearity is listed in Table 1 together with their main physicochemical characteristics. For small clusters,  $\text{Pd}_2\text{CO}$  to  $\text{Pd}_5\text{CO}$ , singlet states are found to be the most stable. For these, the favoured coordination mode is one that promotes the back-bonding interaction, i.e. the capped position ( $\mu_3$ ) on a cluster's face. For larger nuclearities ( $\text{Pd}_6\text{CO}$  to  $\text{Pd}_9\text{CO}$ ), the triplet and quintet states become more stable, favouring vertex coordination. This is because the presence of one ligand is no longer sufficient to offset the stability of the cluster triplet state. To summarize the situation, it is more advantageous for the system to maintain a higher spin state in ways that promote the metal–metal bonds at the expense of lowering metal–ligand bonds rather than switching to a singlet state which would promote the stabilizing interaction with only one ligand at the expense of a large number of metal–metal bonds. To sum up the dual influence to palladium clusters vs. ligands: The singlet state promotes the metal–ligand bond and disadvantages the metal–metal bond while the triplet state promotes the metal–metal bond and disadvantages the metal–ligand bond. This problem will off course

not arise when ligands saturate the cluster and the ground singlet state should occur. The addition of the CO ligand to the cluster induces deformations of the metal skeleton. This could lead to a deltahedral structure, differing from the bare cluster. This is particularly the case for  $\text{Pd}_6$ , where the bare cluster presents an octahedral ground state while the addition of the CO ligand leads to a capped trigonal bipyramid. These two structures can be easily connected by a single normal mode of vibration. Heptamers present similar trends as the bare clusters present a pentagonal bipyramidal ground state while the capped octahedron become the ground state for the monocarbonyl cluster. Note finally that low coordination modes ( $\mu_1$  and  $\mu_2$ ) are expected with the increasing number of ligands. This can be proven experimentally<sup>[3]</sup> and theoretically.<sup>[15]</sup> Regarding the CO ligand, its physicochemical characteristics, bond length ( $d_{\text{Pd-CO}}$ ) and stretching vibration ( $\nu_{\text{CO}}$ ), are consistent with the coordination mode and are generally independent of the number of palladium atoms in the clusters. This CO stretching frequency may thus be considered as a good probe of the structural binding of the ligand to the cluster.

## Conclusions

The objective of this work is a theoretical study of palladium clusters  $\text{Pd}_n$  of low nuclearity, ranging between 1 and 9, and their interactions with the carbonyl ligand ( $\text{Pd}_n\text{CO}$ ). The interaction between the CO ligand and the palladium monomer, dimer and trimer serves to simulate its adsorption on a vertex, an edge and a face of the palladium cluster, respectively. These simulations were conducted using the DFT (B3LYP–Lanl2DZ) approach and have proven to be reliable and comparable to others described in the literature. The step-by-step building of small palladium clusters led us to a series of conclusions, which may be summarized as follows:

- (1) Small palladium clusters ( $\text{Pd}_2$  to  $\text{Pd}_7$ ) are characterized by a triplet ground state. The smaller ones present all deltahedral structures, with distortions more or less important due to the Jahn–Teller effect. For larger nuclearities, the ground spin-multiplicity becomes more important, and  $\text{Pd}_8$  and  $\text{Pd}_9$  have a quintet ground state.
- (2) The study has highlighted the presence of various electronic states relatively close in energy. These states are characterized by quite similar geometries but differ in their electron density distribution. This last point pinpoints the fact that the energy in a series of structural isomers will necessarily be influenced by the choice of the method (the functional and the basis set), so prudence encourages the study of metal clusters by considering, for a given nuclearity, all low-lying minima rather than focusing solely on the global minimum.
- (3) A significant electronic population of the 5s orbital, unoccupied in the atom ground state ( $1^1\text{S-}4\text{d}^{10}$ ), is needed to explain the existence and cohesion of palladium–palladium bonds. The latter are formed by the combination of sd type hybrid orbitals and will get even stronger as the 5s character

increases. This results in a shortening of the bond length with an increase in the average 5s population.

(4) The relative stability of palladium clusters increases with their nuclearity, and the study of fragmentation reactions shows a particular stability of Pd<sub>4</sub>, Pd<sub>6</sub> and Pd<sub>9</sub> clusters.

(5) The adsorption of the CO ligand on palladium clusters goes through a back-bonding interaction. In order to promote this interaction with the ligand, a high 4d population and a low 5s population will be necessary. This interaction therefore affects the metal–metal bond, and the ground state of the cluster becomes a singlet. The favoured coordination mode is one that promotes the back-bonding interaction, i.e. the capped position ( $\mu_3$ ) on a cluster's face. However, stabilization provided by the presence of one ligand at the expense of a large number of metal–metal bonds is not sufficient and, in the case of larger clusters, a larger number of ligands is required.

**Supporting Information** (see footnote on the first page of this article): Cartesian coordinates of the various structures presented in Table 1.

## Acknowledgments

This work was supported by the Belgian Fonds pour la Formation à la Recherche dans l'Industrie et dans l'Agriculture (FRIA-F.N.R.S.) (fellowship to G. Z.). F.R.S.-F.N.R.S. provided access to computational facilities (Project FRFC N°2.4502.05 "Simulation numérique. Application en physique de l'état solide, océanographie et dynamique des fluides").

- [1] R. L. Johnston, *Philos. Trans. R. Soc. Lond., Ser. A* **1998**, 356, 211–230.
- [2] K. Sattler, J. Mühlback, E. Recknagel, *Phys. Rev. Lett.* **1980**, 45, 821–824.
- [3] A. D. Burrows, D. M. P. Mingos, *Transition Met. Chem.* **1993**, 18, 129–148.
- [4] I. Efremenko, M. Sheintuch, *J. Mol. Catal. A* **2000**, 160, 445–451.
- [5] J. Rogan, G. Garcia, J. A. Valdivia, W. Orellana, A. H. Romero, R. Ramirez, M. Kiwi, *Phys. Rev. B* **2005**, 72, 115421–115425.
- [6] G. L. Estiu, M. C. Zemer, *J. Phys. Chem.* **1994**, 98, 4793–4799.
- [7] J. M. Seminario, A. G. Zacarias, M. Castro, *Int. J. Quantum Chem.* **1997**, 61, 515–523.
- [8] W. Zhang, Q. Ge, L. Wang, *J. Chem. Phys.* **2003**, 118, 5793–5801.
- [9] M. Moseler, H. Hakkinen, R. N. Barnett, U. Landman, *Phys. Rev. Lett.* **2001**, 86, 2545–2548.
- [10] G. Zacarias, M. Castro, M. Tour, M. Seminario, *J. Phys. Chem. A* **1999**, 103, 7692–7700.
- [11] P. Nava, M. Sierka, R. Ahlrichs, *Phys. Chem. Chem. Phys.* **2003**, 5, 3372–3381.
- [12] C. Luo, C. Zhou, J. Wu, T. J. D. Kumar, N. Balakrishnan, R. C. Forrey, H. Cheng, *Int. J. Quantum Chem.* **2007**, 107, 1633–1641.
- [13] M. Büyükkata, J. C. Belchior, *Croat. Chem. Acta* **2008**, 81, 289–297.
- [14] V. Bertin, E. Agacino, R. Lopez-Rendon, E. Poulain, *THEO-CHEM* **2006**, 796, 243–248.
- [15] P. Nava, M. Sierka, R. Ahlrichs, *Phys. Chem. Chem. Phys.* **2004**, 6, 5338–5346.
- [16] A. Rochefort, R. Fournier, *J. Phys. Chem.* **1996**, 100, 13506–13513.
- [17] G. Valerio, H. Toulhoat, *J. Phys. Chem. A* **1997**, 101, 1969–1974.
- [18] B. Huber, H. Hakkinen, U. Landman, M. Moseler, *Comput. Mater. Sci.* **2006**, 35, 371–374.
- [19] V. Bertani, C. Cavallotti, M. Masi, S. Carrà, *J. Phys. Chem. A* **2000**, 104, 11390–11397.
- [20] R. G. Parr, W. Yang in *Density-Functional Theory of Atoms and Molecules*, Oxford Science Publications, **1989**.
- [21] A. D. Becke, *J. Chem. Phys.* **1993**, 98, 5648–5652.
- [22] P. J. Hay, W. R. Wadt, *J. Chem. Phys.* **1985**, 82, 270–283.
- [23] P. J. Hay, W. R. Wadt, *J. Chem. Phys.* **1985**, 82, 284–298.
- [24] P. J. Hay, W. R. Wadt, *J. Chem. Phys.* **1985**, 82, 299–310.
- [25] C. Xiao, S. Krüger, T. Belling, M. Mayer, N. Rösch, *Int. J. Quantum Chem.* **1999**, 74, 405–416.
- [26] A. Rassolov, M. A. Ratner, J. A. Pople, P. C. Redfern, L. A. Curtiss, *J. Comput. Chem.* **2001**, 22, 976–984.
- [27] A. E. Reed, R. B. Weinstock, F. Weinhold, *J. Chem. Phys.* **1985**, 83, 735–746.
- [28] A. E. Reed, L. A. Curtiss, F. Weinhold, *Chem. Rev.* **1988**, 88, 899–926.
- [29] M. J. Frisch, G. W. Trucks, H. B. Schlegel, G. E. Scuseria, M. A. Robb, J. R. Cheeseman, J. A. Montgomery Jr., T. Vreven, K. N. Kudin, J. C. Burant, J. M. Millam, S. S. Iyengar, J. Tomasi, V. Barone, B. Mennucci, M. Cossi, G. Scalmani, N. Rega, G. A. Petersson, H. Nakatsuji, M. Hada, M. Ehara, K. Toyota, R. Fukuda, J. Hasegawa, M. Ishida, T. Nakajima, Y. Honda, O. Kitao, H. Nakai, M. Klene, X. Li, J. E. Knox, H. P. Hratchian, J. B. Cross, V. Bakken, C. Adamo, J. Jaramillo, R. Gomperts, R. E. Stratmann, O. Yazyev, A. J. Austin, R. Cammi, C. Pomelli, J. W. Ochterski, P. Y. Ayala, K. Morokuma, G. A. Voth, P. Salvador, J. J. Dannenberg, V. G. Zakrzewski, S. Dapprich, A. D. Daniels, M. C. Strain, O. Farkas, D. K. Malick, A. D. Rabuck, K. Raghavachari, J. B. Foresman, J. V. Ortiz, Q. Cui, A. G. Baboul, S. Clifford, J. Cioslowski, B. B. Stefanov, G. Liu, A. Liashenko, P. Piskorz, I. Komaromi, R. L. Martin, D. J. Fox, T. Keith, M. A. Al-Laham, C. Y. Peng, A. Nanayakkara, M. Challacombe, P. M. W. Gill, B. Johnson, W. Chen, M. W. Wong, C. Gonzalez, J. A. Pople, *Gaussian 03*, Revision C.02, **2004**.
- [30] K. Balasubramanian, *J. Chem. Phys.* **1988**, 89, 6310–6315.
- [31] K. Balasubramanian, *J. Chem. Phys.* **1989**, 91, 307–313.
- [32] D. Dai, K. Balasubramanian, *J. Chem. Phys.* **1995**, 103, 648–655.
- [33] M. Filatov, *Chem. Phys. Lett.* **2003**, 373, 131–135.
- [34] N. R. Walker, J. K.-H. Hui, M. C. L. Gerry, *J. Phys. Chem. A* **2002**, 106, 5803–5808.
- [35] H. Barsch, D. Cohen, S. Topiol, *Isr. J. Chem.* **1980**, 19, 233–241.
- [36] M. D. Morse, *Chem. Rev.* **1986**, 86, 1049–1109.
- [37] Q. Cui, D. G. Musaev, K. Morokuma, *J. Phys. Chem. A* **1998**, 102, 6373–6384.
- [38] J. Moc, D. G. Musaev, K. Morokuma, *J. Phys. Chem. A* **2003**, 107, 4929–4939.
- [39] D. Dai, K. Balasubramanian, *Chem. Phys. Lett.* **1999**, 310, 303–312.
- [40] M. Karabacak, S. Özçelik, Z. B. Güvenç, *Acta Phys. Slovaca* **2004**, 54, 233–244.

Received: June 9, 2009  
Published Online: July 30, 2009